

Dynamic Interface-Assisted Rapid Self-Assembly of DNA Origami-Framed Anisotropic Nanoparticles

Yanfei Qu,[†] Fengyun Shen,[†] Hongzhen Peng, Guifang Chen, Lihua Wang,* and Lele Sun*



Cite This: *JACS Au* 2024, 4, 903–907



Read Online

ACCESS |



Metrics & More



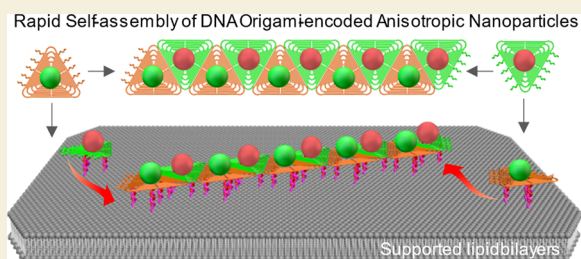
Article Recommendations



Supporting Information

ABSTRACT: The ordered arrangement of nanoparticles can generate unique physicochemical properties, rendering it a pivotal direction in the field of nanotechnology. DNA-based chemical encoding has emerged as an unparalleled strategy for orchestrating precise and controlled nanoparticle assemblies. Nonetheless, it is often time-consuming and has limited assembly efficiency. In this study, we developed a strategy for the rapid and ordered assembly of DNA origami-framed nanoparticles assisted by dynamic interfaces. By assembling Au nanoparticles (AuNPs) onto DNA origami with different sticky ends in various directions, we endowed them with anisotropic specific affinities. After assembling DNA origami-framed AuNPs onto supported lipid bilayers with freely diffusing single-stranded DNA via DNA hybridization, we found that DNA origami-framed AuNPs could form larger ordered assemblies than those in 3D solution within equivalent time frames. Furthermore, we also achieved rapid and ordered assembly of liposome nanoparticles by employing the aforementioned strategy. Our work provides a novel avenue for efficient and rapid assembly of nanoparticles across two-dimensional interfaces, which is expected to promote the application of ordered nanoparticle assemblies in sensor and biomimetic system construction.

KEYWORDS: Self-assembly, DNA, Nanoparticles, Lipid bilayers, Interface



INTRODUCTION

The self-assembly of nanoparticles into ordered structures is of significant importance for harnessing the excellent physicochemical properties of nanomaterials.^{1–3} Although van der Waals forces, electrostatic interactions, hydrogen bonds, molecular dipole interactions, and DNA base pairing can drive the ordered arrangement of nanoparticles,^{4,5} it is challenging to assemble nanoparticles into customized morphologies along controlled pathways. The advancement of structural DNA nanotechnology has facilitated the controllable assembly of nanoparticles.^{6–11} On one hand, by leveraging the addressability of DNA nanostructures, DNA-modified nanoparticles can be assembled onto individual DNA nanostructures with controlled copy numbers and spacing;^{12–14} on the other hand, DNA nanostructures can encode individual nanoparticles, enabling them to acquire anisotropic specific affinity, thereby allowing nanoparticles to assemble into arrays along predefined pathways.^{15–17} However, in a solution environment, the assembly rate of the DNA nanostructures themselves, as well as DNA nanostructure-encoded nanoparticles, is relatively slow. Stringent annealing conditions and several tens of hours are often required to obtain arrays with the desired morphology.¹⁸

In recent years, research on the interaction between DNA nanostructures and solid supported lipid bilayers (SLBs) have inspired innovative approaches to fabricating DNA nanoarrays.^{19–22} DNA nanostructures can bind onto SLBs through

various pathways.^{20,21,23} One approach involves the electrostatic adsorption of DNA nanostructures mediated by divalent metal ions to zwitterionic bilayers.²⁰ Another approach entails the hybridization of anchoring DNA chains on DNA nanostructures with the single-stranded DNA (ssDNA) on the surface of SLBs.²¹ Additionally, DNA nanostructures can also be embedded into phospholipid bilayers through lipid molecules carried by themselves, such as cholesterol.²³ Biological membranes can confine membrane-bound proteins in 2D space, thereby increasing the probability of their interactions. Therefore, DNA nanostructures bound to SLBs should also be able to self-assemble into higher-order structures more efficiently compared to in a 3D solution environment, as evidenced by multiple studies.^{20,24} For example, cross-shaped DNA origami units with dimensions of 64 nm in length and width can form micrometer-scale 2D arrays on SLBs composed of zwitterionic 1,2-dioleoyl-*sn*-glycero-3-phosphocholine (DOPC) within minutes in the presence of Mg²⁺.²⁰

Received: February 17, 2024

Revised: March 4, 2024

Accepted: March 6, 2024

Published: March 8, 2024



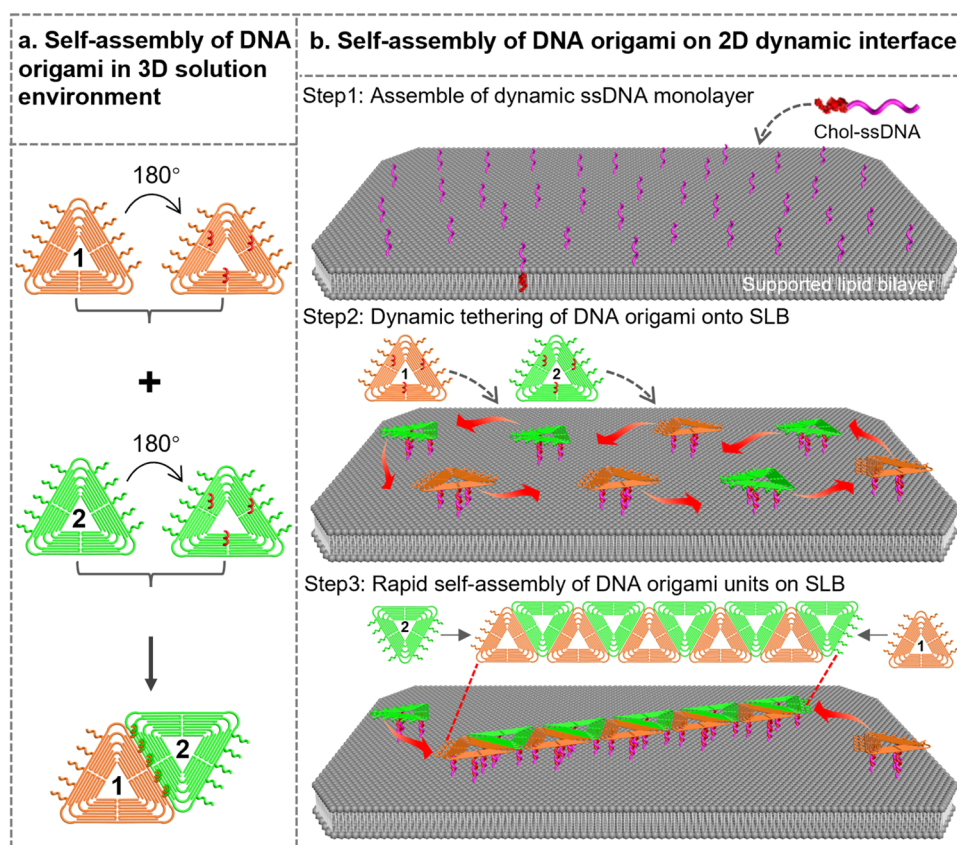


Figure 1. Schematic showing the design of triangular DNA origami Units 1 and 2 (a) and 2D dynamic interface (SLBs)-assisted rapid self-assembly of Units 1 and 2. Chol-ssDNA: cholesterol-modified ssDNA.

Therefore, in this study, we proposed the use of SLBs as a dynamic interface to assist the rapid self-assembly of DNA origami-framed anisotropic nanoparticles. We first employed triangular DNA origami to encode gold nanoparticles (AuNPs) and liposomes with anisotropic affinities and then assembled the triangular origami-framed anisotropic AuNPs onto fluidic SLBs through DNA hybridization. We found that the triangular DNA origami-framed anisotropic AuNPs assembled on SLBs could undergo free two-dimensional diffusion and form 1D arrays with lengths exceeding one micron within 2 h. In comparison, in a solution environment, assemblies formed by only 2–5 triangular DNA origami-framed AuNPs were observed within the same time frame. Furthermore, we also realized the rapid self-assembly of DNA origami-framed liposomes on SLBs with the strategy described above. Therefore, our work provided a novel strategy for the rapid preparation of inorganic and organic nanoparticle arrays on two-dimensional interfaces, holding significant potential for applications in sensor and biomimetic system construction.

RESULTS AND DISCUSSION

Before attempting to promote the self-assembly of DNA origami-framed anisotropic nanoparticles using SLBs, we planned to first compare the differences in the self-assembly efficiency of DNA origamis themselves on SLBs and in solution environments. As shown in Figures 1 and S1, we designed two types of DNA origami units (units 1 and 2) based on previously reported triangular DNA origami. Each unit had five protruding arm chains on both the A and B sides (U1A1–U1A5, U1B1–U1B5, U2A1–U2A5, U2B1–U2B5)

for the assembly of Unit 1 and Unit 2. Of note, arm chains U1A1, U1A2, U1A3, U1A4, and U1A5 on Unit 1 could specifically hybridize with arm chains U2A5, U2A4, U2A3, U2A2, and U2A1 on Unit 2, respectively; while arm chains U1B1, U1B2, U1B3, U1B4, and U1B5 could specifically hybridize with arm chains U2B5, U2B4, U2A3, U2A2, and U2A1 on Unit 2, respectively; thereby mediating the self-assembly of Unit 1 and Unit 2 into one-dimensional arrays. Additionally, to assemble Units 1 and 2 onto SLBs and enable their free diffusion, we designed three anchoring chains on each unit which could hybridize with the cholesterol-modified ssDNA embedded in the SLBs. The reason we designed three anchoring chains was that according to our previous studies, more anchoring chains may reduce the diffusion rate of DNA origami on SLBs, potentially affecting the efficiency of self-assembly.²⁵

Then, we planned to use atomic force microscopy (AFM) imaging to demonstrate whether Unit 1 and Unit 2 exhibit higher self-assembly efficiency on the SLBs. For this purpose, we first prepared liposomes containing DOPC and 1,2-dipalmitoyl-*sn*-glycero-3-phosphocholine (DPPC) (molar ratio of DOPC:DPPC = 70:30), and we further prepared SLBs by incubating liposomes with clean mica surfaces. The choice of liposomes containing DOPC and DPPC for SLBs preparation was because the difference in phase transition temperatures between the two phospholipids could lead to phase separation. Additionally, due to the difference in molecular structures, the height of the regions where DPPC aggregated would be higher, which aided our in determining the formation of SLBs via AFM imaging (Figure S2). Upon the formation of SLBs, incubation of cholesterol-modified ssDNA

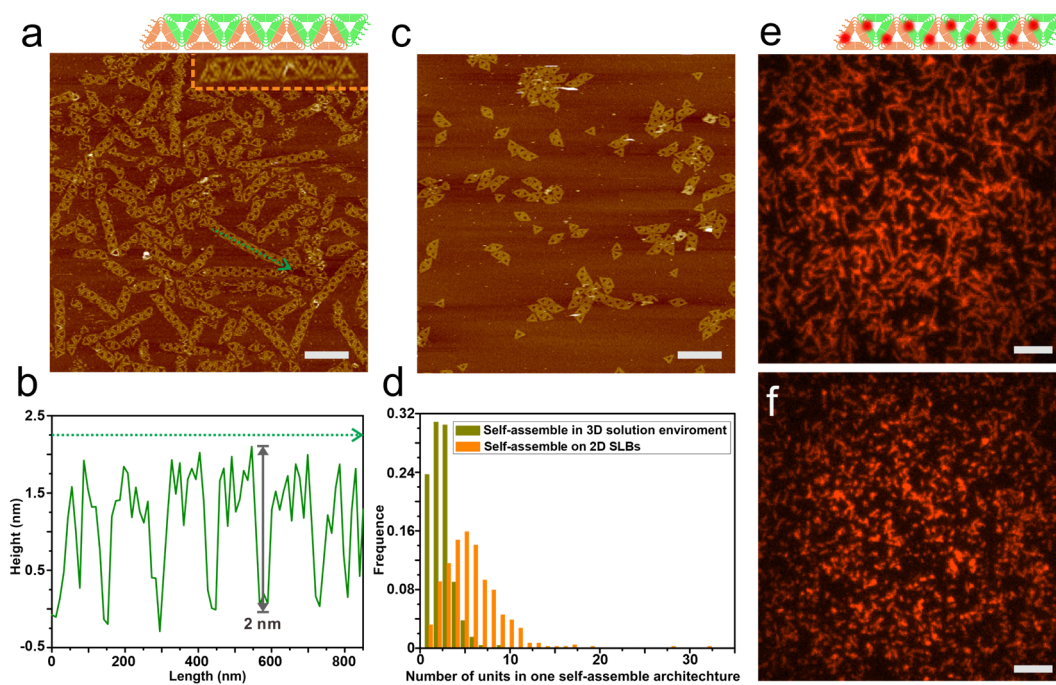


Figure 2. (a,b) Atomic force microscopy imaging results of the self-assembly of Units 1 and 2 on the SLBs (a) and representative height maps of 1D DNA origami arrays (b). (c) Atomic force microscopy imaging results of the self-assembly of Units 1 and 2 in a solution environment. (d) Histogram of the frequency distribution of the number of DNA origami units in self-assembled structures under different conditions. (e,f) TIRFM imaging results of the self-assembly of Units 1 and 2 on the SLBs (e) and in solution (f). Scale bar is 200 nm in parts a and c; scale bar is 3 μm in parts e and f.

with the SLBs resulted in the formation of freely diffusing DNA monolayers on the SLBs, as demonstrated in our previous study.²⁵ Subsequently, through AFM imaging, we demonstrated that Unit 1 and Unit 2 could be assembled onto the SLBs through DNA hybridization and form linear assemblies comprising more than ten DNA origami units within 2 h (Figures 2a,b,d and S3). In contrast, in a solution environment, incubation of both Unit 1 and Unit 2 in a 1:1 molar ratio for 2 h only resulted in the formation of assemblies mostly consisting of up to five monomers (Figure 2c,d).

Furthermore, we labeled Unit 1 and Unit 2 with fluorescent molecules (Cy3) and observed their self-assembly on SLBs by using total internal reflection fluorescence microscopy (TIRFM) (Figure S1). In this part, SLBs were prepared on the glass bottom of clean cell culture dishes. Similarly, fluorescently labeled DNA origami could be specifically assembled onto SLBs via DNA hybridization (Figure S4). Moreover, when only one type of Unit was assembled on the SLBs or when both Units were assembled but lacked arm chains, we observed only discrete spots of fluorescence (Figure S5). Furthermore, when both Unit 1 and Unit 2 were coincubated with SLBs, numerous linear spots of fluorescence with lengths exceeding one micron were observed after approximately one h (Figure 2e). However, when Unit 1 and Unit 2 were first incubated in solution for 1 h and then transferred to SLBs for immediate observation, no significant linear spots of fluorescence were observed (Figure 2f). These results indicated that indeed DNA origami could self-assemble more rapidly on SLBs.

Next, we attempted to utilize SLBs to promote the assembly of DNA origami-framed AuNPs. As shown in Figure 3a, for real-time observation of the assembly process using TIRFM, we prepared two types of ssDNA-modified AuNPs, one labeled

with Cy3 and the other labeled with carboxyfluorescein (FAM). Cy3-labeled AuNPs and FAM-labeled AuNPs could be respectively assembled onto Units 1 and 2 through DNA hybridization (Figure S6), thus enabling us to observe whether the two types of AuNPs assembled together to form 1D arrays on SLBs through fluorescence colocalization. Prior to this, we demonstrated that both 15 and 30 nm AuNPs could be efficiently assembled onto triangular DNA origami through AFM imaging (Figure S7). Additionally, AFM imaging results also confirmed that Unit 1- and Unit 2-framed AuNPs could form linear assemblies in a solution environment, but with low efficiency. Only assemblies consisting of 2–5 units were formed within 24 h (Figures S8 and S9).

Subsequently, through TIRFM imaging, we found that Unit 1- and Unit 2-framed AuNPs could also be specifically assembled onto the SLBs through DNA hybridization (Figure S10). Moreover, the DNA origami-framed AuNPs could freely move on the SLBs (SI Video). After simultaneously assembling Unit 1- and Unit 2-framed 15 nm AuNPs onto the SLBs, we conducted a real-time observation of the assembly process. It was found that both types of AuNPs were dispersed on the SLBs at 0 min. However, after 120 min, the spots of both types of AuNPs aggregated into linear shapes, and the fluorescence from FAM and Cy3 could be colocalized (Figure 3b). This was because after self-assembly of Unit 1- and Unit 2-framed AuNPs into linear arrays, their diffusion rate on the SLBs became very slow. As a control, if only Unit 1- or Unit 2-framed AuNPs were assembled on the SLBs, the fluorescent spots of AuNPs remained dispersed (Figure S11). Additionally, we found that Unit 1- or Unit 2-framed 30 nm AuNPs could also efficiently assemble into linear arrays on the SLBs (Figure 3c).

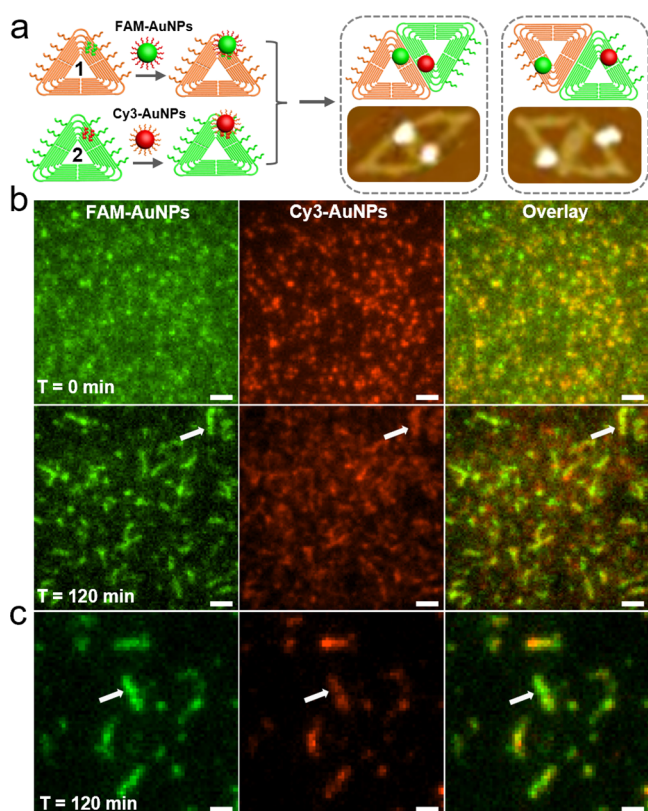


Figure 3. (a) Schematic showing the design of DNA origami-framed AuNPs, and representative AFM images showing the self-assembly of Unit 1- and Unit 2-framed AuNPs. (b,c) TIRFM imaging demonstrating the self-assembly of Unit 1- and Unit 2-framed 15 nm AuNPs (b) and 30 nm AuNPs (c) on SLBs at different time points. Scale bars in b and c are 2 and 1 μm , respectively.

Next, we planned to adopt the strategy described above in the self-assembly of DNA origami-framed lipid nanoparticles. To achieve this, we first prepared liposomes with a diameter of 50 nm labeled with 1,2-dimyristoyl-*sn*-glycero-3-phosphoethanolamine-*N*-(7-nitro-2-1,3-benzoxadiazol-4-yl) (NBD) (excited by 488 nm laser), and then modified liposomes with cholesterol-labeled ssDNA (Figure S12). To assemble the liposomes onto Units 1 and 2, we designed 12 arm DNA chains on the inner side of Units 1 and 2 (Figure S13), which were complementary to the ssDNA on the liposomes. Additionally, we decorated each Unit 1 and Unit 2 with one Cy3 for observing the assembly of Unit 1- and Unit 2-framed liposomes using TIRFM (Figure 4a). After simultaneously assembling Unit 1- and Unit 2-framed liposomes onto the SLBs, we found that after 60 min, Unit 1- and Unit 2-framed liposomes could assemble into small-sized linear arrays, as indicated by colocalized linear fluorescence spots of Cy3 and NBD. By 180 min, Unit 1- and Unit 2-framed liposomes assembled into larger-sized linear arrays (Figure 4b). These results indicated that SLBs could also promote the rapid self-assembly of DNA origami-framed lipid nanoparticles.

CONCLUSION

In conclusion, this study developed a strategy for the rapid and ordered assembly of DNA origami-framed nanoparticles assisted by fluidic supported lipid bilayers (SLBs) as dynamic interfaces. By employing triangular DNA origami to encode both gold nanoparticles (AuNPs) and liposomes with

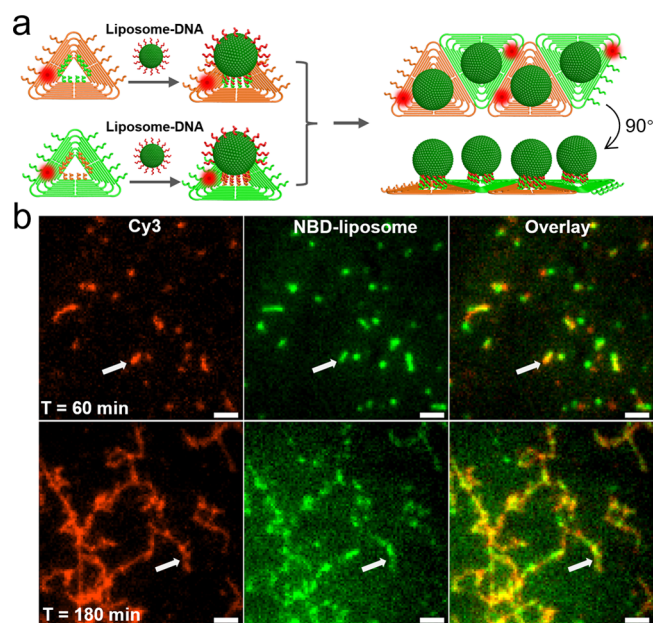


Figure 4. (a) Schematic showing the design of DNA origami-framed liposomes and their self-assembly. (b) TIRFM imaging demonstrating the self-assembly of Unit 1- and Unit 2-framed liposome on SLB at different time point. Scale bar: 2 μm .

anisotropic affinities, we successfully realized the rapid self-assembly of these nanoparticles on fluidic SLBs. Notably, our findings demonstrated that the DNA origami-framed anisotropic nanoparticles assembled on SLBs could form 1D arrays exceeding one micron in length within a remarkably short time frame of 2 h, surpassing the assembly outcomes observed in solution environments. By providing a streamlined method for the rapid preparation of both inorganic and organic nanoparticle arrays on two-dimensional interfaces, our work opens avenues for advancing the development of nanotechnology-enabled devices and systems.

ASSOCIATED CONTENT

Supporting Information

The Supporting Information is available free of charge at <https://pubs.acs.org/doi/10.1021/jacsau.4c00145>.

Additional experimental details, materials, and methods, including photographs of experimental setup (PDF)
Movie showing movement of DNA origami-framed AuNPs on SLBs (MP4)

AUTHOR INFORMATION

Corresponding Authors

Lele Sun – Institute of Materiobiology, Department of Chemistry, College of Science, Shanghai University, Shanghai 200444, China; orcid.org/0000-0002-8052-9451; Email: sunlele@shu.edu.cn

Lihua Wang – Institute of Materiobiology, Department of Chemistry, College of Science, Shanghai University, Shanghai 200444, China; Email: wanglihua@shu.edu.cn

Authors

Yanfei Qu – School of Life Science, Shanghai University, Shanghai 200444, China; Institute of Materiobiology,

Department of Chemistry, College of Science, Shanghai University, Shanghai 200444, China

Fengyun Shen – Institute of Materiobiology, Department of Chemistry, College of Science, Shanghai University, Shanghai 200444, China

Hongzhen Peng – Institute of Materiobiology, Department of Chemistry, College of Science, Shanghai University, Shanghai 200444, China

Guifang Chen – School of Life Science, Shanghai University, Shanghai 200444, China; orcid.org/0000-0002-4470-9105

Complete contact information is available at:
<https://pubs.acs.org/10.1021/jacsau.4c00145>

Author Contributions

[†]Y.Q. and F.S. contributed equally. L.S., Y.Q., and F.S. conducted the experiment. All authors contributed to data analysis and writing of the manuscript. L.S. and L.W. offered funding acquisition. CRediT: **Yanfei Qu** data curation, formal analysis, investigation, methodology, validation, writing-original draft; **Fengyun Shen** data curation, investigation, methodology; **Guifang Chen** supervision; **Lihua Wang** supervision; **Lele Sun** conceptualization, funding acquisition, supervision, writing-original draft, writing-review & editing.

Notes

The authors declare no competing financial interest.

ACKNOWLEDGMENTS

This work was partially supported by the National Key Research and Development Program of China (2023YFB3507700, 2022YFB3808200) and the National Natural Science Foundation of China (22277071).

REFERENCES

- (1) Grzelczak, M.; Vermant, J.; Furst, E. M.; Liz-Marzan, L. M. Directed Self-Assembly of Nanoparticles. *ACS Nano* **2010**, *4* (7), 3591–3605.
- (2) Thorkelsson, K.; Bai, P.; Xu, T. Self-assembly and applications of anisotropic nanomaterials: A review. *Nano Today* **2015**, *10* (1), 48–66.
- (3) Deng, K.; Luo, Z.; Tan, L.; Quan, Z. Self-assembly of anisotropic nanoparticles into functional superstructures. *Chem. Soc. Rev.* **2020**, *49* (16), 6002–6038.
- (4) Lim, S. I.; Zhong, C.-J. Molecularly Mediated Processing and Assembly of Nanoparticles: Exploring the Interparticle Interactions and Structures. *Acc. Chem. Res.* **2009**, *42* (6), 798–808.
- (5) Luo, D.; Yan, C.; Wang, T. Interparticle Forces Underlying Nanoparticle Self-Assemblies. *Small* **2015**, *11* (45), 5984–6008.
- (6) Seeman, N. C.; Sleiman, H. F. DNA nanotechnology. *Nat. Rev. Mater.* **2018**, *3* (1), 17068.
- (7) Zhang, F.; Nangreave, J.; Liu, Y.; Yan, H. Structural DNA Nanotechnology: State of the Art and Future Perspective. *J. Am. Chem. Soc.* **2014**, *136* (32), 11198–11211.
- (8) Madsen, M.; Gothelf, K. V. Chemistries for DNA Nanotechnology. *Chem. Rev.* **2019**, *119* (10), 6384–6458.
- (9) Chen, Y.; Chen, X.; Zhang, B.; Zhang, Y.; Li, S.; Liu, Z.; Gao, Y.; Zhao, Y.; Yan, L.; Li, Y.; Tian, T.; Lin, Y. DNA framework signal amplification platform-based high-throughput systemic immune monitoring. *Signal Transduct. Target. Ther.* **2024**, *9* (1), 28–28.
- (10) Tian, T.; Zhang, T.; Shi, S.; Gao, Y.; Cai, X.; Lin, Y. A dynamic DNA tetrahedron framework for active targeting. *Nat. Protoc.* **2023**, *18* (4), 1028–1055.
- (11) Zhang, T.; Ma, H.; Zhang, X.; Shi, S.; Lin, Y. Functionalized DNA Nanomaterials Targeting Toll-Like Receptor 4 Prevent

Bisphosphonate-Related Osteonecrosis of the Jaw via Regulating Mitochondrial Homeostasis in Macrophages. *Adv. Funct. Mater.* **2023**, *33* (15), 202213401.

(12) Kou, B.; Wang, Z.; Mousavi, S.; Wang, P.; Ke, Y. Dynamic Gold Nanostructures Based on DNA Self Assembly. *Small* **2023**, DOI: 10.1002/smll.202308862.

(13) Wang, Z.-G.; Ding, B. Engineering DNA Self-Assemblies as Templates for Functional Nanostructures. *Acc. Chem. Res.* **2014**, *47* (6), 1654–1662.

(14) Keller, A.; Linko, V. Challenges and Perspectives of DNA Nanostructures in Biomedicine. *Angew. Chem.-Int. Ed.* **2020**, *59* (37), 15818–15833.

(15) Hu, Y.; Niemeyer, C. M. From DNA Nanotechnology to Material Systems Engineering. *Adv. Mater.* **2019**, *31* (26), 1806294.

(16) Liu, W.; Halverson, J.; Tian, Y.; Tkachenko, A. V.; Gang, O. Self-organized architectures from assorted DNA-framed nanoparticles. *Nat. Chem.* **2016**, *8* (9), 867–873.

(17) Tan, L. H.; Xing, H.; Lu, Y. DNA as a Powerful Tool for Morphology Control, Spatial Positioning, and Dynamic Assembly of Nanoparticles. *Acc. Chem. Res.* **2014**, *47* (6), 1881–1890.

(18) Pinheiro, A. V.; Han, D.; Shih, W. M.; Yan, H. Challenges and opportunities for structural DNA nanotechnology. *Nat. Nanotechnol.* **2011**, *6* (12), 763–772.

(19) Suzuki, Y.; Kawamata, I.; Watanabe, K.; Mano, E. Lipid bilayer-assisted dynamic self-assembly of hexagonal DNA origami blocks into monolayer crystalline structures with designed geometries. *iScience* **2022**, *25* (5), 104292.

(20) Suzuki, Y.; Endo, M.; Sugiyama, H. Lipid-bilayer-assisted two-dimensional self-assembly of DNA origami nanostructures. *Nat. Commun.* **2015**, *6*, 8052.

(21) Kocabay, S.; Kempter, S.; List, J.; Xing, Y.; Bae, W.; Schiffels, D.; Shih, W. M.; Simmel, F. C.; Liedl, T. Membrane-Assisted Growth of DNA Origami Nanostructure Arrays. *ACS Nano* **2015**, *9* (4), 3530–3539.

(22) Khmelinskaja, A.; Franquelim, H. G.; Yaadav, R.; Petrov, E. P.; Schwille, P. Membrane-Mediated Self-Organization of Rod-Like DNA Origami on Supported Lipid Bilayers. *Adv. Mater. Interfaces* **2021**, *8* (24), 2101094.

(23) Langecker, M.; Arnaut, V.; List, J.; Simmel, F. C. DNA Nanostructures Interacting with Lipid Bilayer Membranes. *Acc. Chem. Res.* **2014**, *47* (6), 1807–1815.

(24) Julin, S.; Keller, A.; Linko, V. Dynamics of DNA Origami Lattices. *Bioconjugate Chem.* **2023**, *34* (1), 18–29.

(25) Sun, L.; Gao, Y.; Xu, Y.; Chao, J.; Liu, H.; Wang, L.; Li, D.; Fan, C. Real-Time Imaging of Single-Molecule Enzyme Cascade Using a DNA Origami Raft. *J. Am. Chem. Soc.* **2017**, *139* (48), 17525–1753.